

ChemComm

Accepted Manuscript



This is an *Accepted Manuscript*, which has been through the Royal Society of Chemistry peer review process and has been accepted for publication.

Accepted Manuscripts are published online shortly after acceptance, before technical editing, formatting and proof reading. Using this free service, authors can make their results available to the community, in citable form, before we publish the edited article. We will replace this *Accepted Manuscript* with the edited and formatted *Advance Article* as soon as it is available.

You can find more information about *Accepted Manuscripts* in the [Information for Authors](#).

Please note that technical editing may introduce minor changes to the text and/or graphics, which may alter content. The journal's standard [Terms & Conditions](#) and the [Ethical guidelines](#) still apply. In no event shall the Royal Society of Chemistry be held responsible for any errors or omissions in this *Accepted Manuscript* or any consequences arising from the use of any information it contains.

Cite this: DOI: 10.1039/c0xx00000x

www.rsc.org/xxxxxx

ARTICLE TYPE

Molecular brass: Cu₄Zn₄, A ligand protected superatom cluster.Kerstin Freitag,^a Hung Banh,^a Christian Gemel,^a Rüdiger W. Seidel^a Samia Kahlal^b, Jean-Yves Saillard,^b and Roland A. Fischer^{a,*}

Received (in XXX, XXX) Xth XXXXXXXXX 20XX, Accepted Xth XXXXXXXXX 20XX

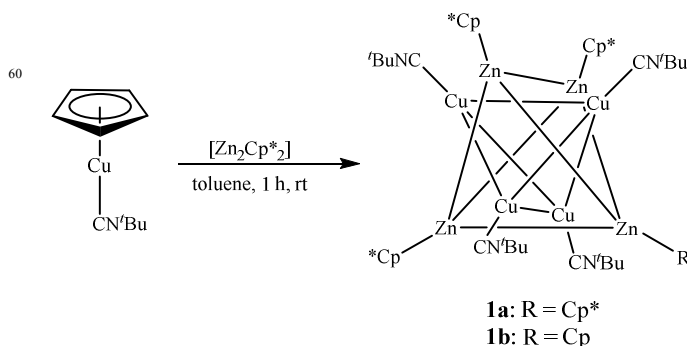
DOI: 10.1039/b000000x

The first example of ligand protected Cu/Zn clusters is described. Reaction of [CpCu(CN^tBu)] with [Zn₂Cp*₂] yields [(CuCN^tBu)₄(ZnCp*)₄] (**1a**) and [(CuCN^tBu)₄(ZnCp*)₃(ZnCu)] (**1b**). According to DFT calculations, the [Cu₄Zn₄] unit fulfils the unified superatom model for cluster valence shell closing.

Brass (Cu/Zn) is one of the longest known and most common alloys and a classic example of a Hume Rothery phase. It is used in various applications, due to its increased heat transfer, strength, hardness and corrosion resistance compared to pure copper. Quite in contrast to many other important alloys and intermetallic compounds, the bottom-up nano chemistry of brass and the properties of Cu/Zn nanoalloys have not been widely studied.¹ In particular, only very few reports have appeared demonstrating the wet chemical synthesis of Cu/Zn nanoparticles by precursor routes.²⁻⁵ For example, co-hydrogenolysis of [CpCu(PMe₃)] and [ZnCp*₂] has been found as a pathway to surfactant stabilized brass nano-particles (Cp = C₅H₅; Cp* = C₅Me₅; Me = CH₃).³ Molecular congeners of nano-brass, i.e. clusters with an atom-precise mixed metal core Cu_aZn_b have not been reported to date. Actually, there is not even a single example of a structurally characterized molecular compound in the literature which structure features an unsupported covalent Cu–Zn bond.⁶ For many years we have been working to develop strategies for the controlled synthesis of ligand protected mixed transition metal (A) main group-12/13 metal (B) coordination compounds and/or clusters of the general formula [A_aB_b]R_c (R = hydrocarbon ligand), being inspired by the compositions and structural motifs of Hume Rothery type intermetallics.⁷ We refer to [MoZn₁₂]R₁₂ and [Pd₂Zn₆Ga₂]R₈ (R = Cp* and Me) as just two important examples which were obtained by transmetallation reactions using [Mo(GaCp*)₆] or [Pd₂(GaCp*)₅] and ZnMe₂ as reagents (Ga/Zn and Cp*/Me exchange).^{8,9} However, this strategy failed when applied to the Cu–Zn target. Alternatively, we found “Carmonas compound” [Zn₂Cp*₂] to be a very flexible reagent for controlled A–Zn bond formation.¹⁰

Herein we report on the synthesis and characterization of the first example of a atom-precise molecular Cu/Zn cluster: two closely related species, namely [(CuCN^tBu)₄(ZnCp*)₄] (**1a**) (^tBu = *tert*-butyl) and [(CuCN^tBu)₄(ZnCp*)₃(ZnCu)] (**1b**) were obtained simultaneously. Treatment of [CpCuCN^tBu] with an *equimolar*

amount of [Zn₂Cp*₂] in toluene at room temperature over a period of 1 h leads to the formation of a dark red solution, from which **1a/1b** co-crystallizes as dark red cubes upon cooling at –30 °C (Scheme 1). The crystals **1a/1b** have to be manually separated from the pale yellow crystals of the by-product [Cp*CuCN^tBu], which was achieved with the aid of an optical microscope in a glovebox under argon atmosphere. In-situ ¹H NMR indicates the formation of two additional by-products, which are identified as the two zincocene complexes [ZnCp*₂] and [ZnCp*Cu]. All attempts to separate **1a** and **1b** from these by-products by washing, re-crystallization from various solvents sublimation or column chromatography remained unsuccessful.



Scheme 1 Formation of the Cu₄Zn₄ clusters [(CuCN^tBu)₄(ZnCp*)₄] (**1a**) and [(CuCN^tBu)₄(ZnCp*)₃(ZnCu)] (**1b**). The illustration of **1a/1b** emphasizes the tetrahedral arrangement of Cu₄ and Zn₄ disregarding the actual bonding situation.

The clusters **1a** and **1b** are isostructural except for the nature of one of the four cyclopentadienyl ligands: In **1a** all four cyclopentadienyl ligands are Cp*, whereas in **1b** one of these ligands is Cp. Notably, [Cp*CuCN^tBu] is not reactive towards [Zn₂Cp*₂] and the combination of these two compounds did, surprisingly, not lead to the anticipated cluster **1a**. Obviously, the reaction of [CpCuCN^tBu] with [Zn₂Cp*₂] involves competitive ligand exchange reactions and is sensitive to ligand variations at the Cu site. The observation of Zn(II) species (ZnR₂, R = Cp, Cp*) indicates a formal redox chemical process, where the Zn(I) of [Zn₂Cp*₂] is oxidized and the Cu(I) of [CpCuCN^tBu] is reduced to Cu(0). Preliminary experiments show that if the reaction is performed in absence of the isonitrile ligand at very low temperature with [Cp*Cu] formed in situ,¹¹ no redox

chemistry is observed. Instead, $[\text{Zn}_2\text{Cp}^*_2]$ simply adds to the fragment $[\text{Cp}^*\text{Cu}]$ leading to the neutral cluster $[\text{Zn}_2\text{Cu}]\text{Cp}^*_3$ with a triangular structure consisting of two ZnCp^* and one CuCp^* vertex, which is currently under investigation. The isolated crystals **1a/1b** are stable under an inert gas atmosphere at $-30\text{ }^\circ\text{C}$ for several weeks, but decompose at room temperature within a few days. The clusters **1a** and **1b** are barely soluble in *n*-hexane, but readily dissolve in other non polar solvents like toluene or benzene. **1a** and **1b** are stable in solution up to $80\text{ }^\circ\text{C}$, but higher temperatures lead to decomposition under formation of a metallic precipitate. The ^1H NMR spectrum of the red crystals **1a/1b** in C_6D_6 at room temperature shows a mixture of **1a** and **1b** in an approximate 1:1 molar ratio (without any further impurities). **1a** gives rise to the expected set of signals for a T_d symmetric cluster, *i.e.* one signal at $\delta = 1.24\text{ ppm}$ (s, 36H) for the *tert*-butyl-isonitrile groups and one signal at $\delta = 2.37\text{ ppm}$ (s, 60H) for the Cp^* ligands. In contrast, **1b** shows only C_{3v} symmetry with two signals for the *tert*-butyl-isonitriles ($\delta = 1.31\text{ ppm}$ (s, 9H), $\delta = 1.32\text{ ppm}$ (s, 27H)) as well as signals for Cp^* ($\delta = 2.36\text{ ppm}$ (s, 45H)) and Cp ($\delta = 6.37\text{ ppm}$ (s, 5H)). ^{13}C NMR data could not be obtained due to the poor solubility of **1a** and **1b**. Liquid injection field desorption ionization mass spectrometry (LIFDI-MS) reveals both $[\text{M}]^+$ ion peaks at m/z [a.u.] = 1389 (**1a**) and 1319 (**1b**), together with various fragment peaks due to the consecutive loss of organic ligands (see Figure 1 and Figure S4)

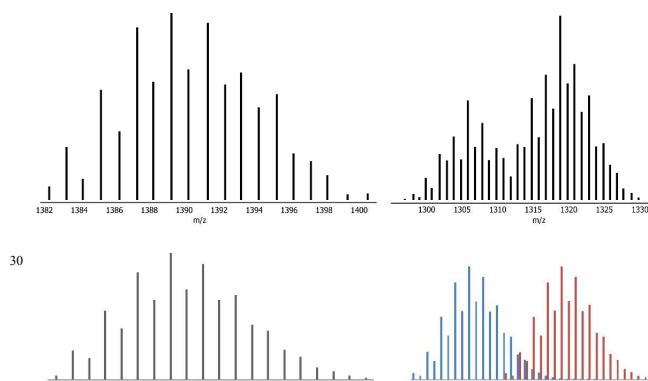


Figure 1. Top left: Molecular ion peak of **1a** ($m/z = 1389$). Top right: Molecular ion peak of **1b** ($m/z = 1319$), superimposed with $[\mathbf{1a}\text{-CN}^t\text{Bu}]^+$ ($m/z = 1306$). Bottom left: Calculated isotopic pattern for $[\mathbf{1a}]^+$. Bottom right: Superimposed calculated isotopic patterns of $[\mathbf{1b}]$ and $[\mathbf{1a}\text{-CN}^t\text{Bu}]^+$.

The ATR-FTIR spectrum of **1a/1b** shows the absorption bands typical of Cp^* units ($2937, 2880, 2829\text{ cm}^{-1}$) and CN^tBu ligands (2104 cm^{-1}). **1a/1b** crystallizes in the cubic space group $I\bar{4}3m$ with the molecules of **1a/1b** located on a $\bar{4}3m$ special position. In accordance with the ^1H NMR and LIFDI-MS data, the refinement of the crystal structure was based on a 1:1 solid solution model of **1a** and **1b**, *i.e.* the clusters share the same site in the crystal structure. Clearly, Cu and Zn as neighbouring elements in the periodic table cannot be distinguished by routine single-crystal X-ray diffraction experiments. However, according to the T_d symmetry of the cluster found in the ^1H NMR spectrum, only two isomeric forms of **1a** and **1b** are possible: either with $\text{ZnCp}^*(\text{Cp})$ and CuCN^tBu coordination or with ZnCN^tBu and $\text{CuCp}^*(\text{Cp})$. An

unambiguous assignment can be made by DFT calculations (see below). It is also possible on the basis of the typical $\nu(\text{CN})$ stretching vibration in the IR spectrum: This band is observed at 2104 cm^{-1} for **1a/1b** which is well comparable with the $\nu(\text{CN})$ stretching vibration found in other CuCN^tBu compounds such as the starting compound $[\text{CpCuCN}^t\text{Bu}]$ (2144 cm^{-1}).¹² This vibration is very close to that of free CN^tBu (2138 cm^{-1}), while it is shifted to much higher wavenumbers in the few known complexes with a ZnCN^tBu unit ($2218\text{-}2244\text{ cm}^{-1}$).¹³ The Cu and Zn content was determined by atomic absorption spectroscopy (calcd. Cu: 18.77, Zn: 19.31 %; found Cu: 19.32, Zn 20.51 %), being in accordance with the assigned 1:1 molar ratio of the two elements. Due to the lack of pure samples of **1a/1b** on a multi milligram scale, no CHN analyses have been carried out. The refined structure of **1a/1b** contains residual electron density ($1.661\text{ e}/\text{\AA}^3$) which might be assigned to disordered toluene (see SI for further information).

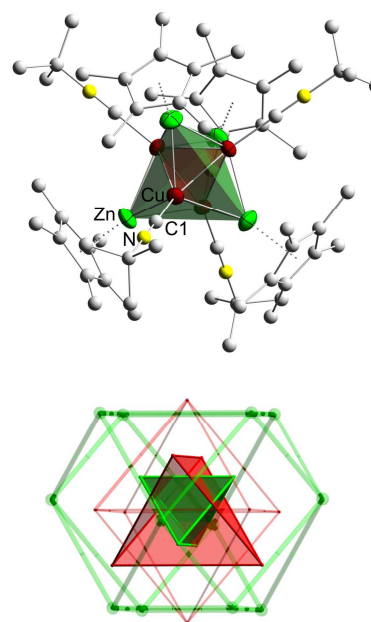


Figure 2 Top: Molecular structure of compound **1a/1b** (red: Cu, green: Zn). Displacement ellipsoids of the metal atoms are drawn at the 30 % probability level. Disordered positions of the Cp^* ligands and hydrogen atoms are omitted for clarity. Selected interatomic distances (\AA) and angles ($^\circ$) for **1a/1b**: Cu-Cu 2.471(4), Cu-Zn 2.498(2), Cu-C1 1.892(1), Zn- Cp^* centroid 2.055, Cu-Cu-Cu 59.99(1), Cu-Zn-Cu 59.29(11), Zn-Cu-Cu 60.35(5). Bottom: $\text{Cu}_{10}\text{Zn}_{16}$ cluster of the γ -brass solid state structure (green: Zn, red: Cu).

The crystallographic site symmetry generates a T_d -symmetric arrangement of the four copper atoms, which form the corners of a Cu_4 tetrahedron with Cu-Cu-Cu angles of 60° . The Cu-Cu distances of $2.471(4)\text{ \AA}$ are longer than the Cu-Cu bond length in $[(\text{IPrCuH})_2]$ ($\text{IPr} = 1,3\text{-bis}(2,6\text{-diisopropylphenyl})\text{imidazol-2-ylidene}$) ($2.305(1)\text{ \AA}$), which is the shortest Cu-Cu bond known so far, but lie within the range of Cu-Cu distances reported for other molecular compounds ($2.305(1) - 3.424(2)\text{ \AA}$).¹⁴⁻¹⁶ Each face of the Cu_4 tetrahedron is capped by a ZnCp^* moiety

resulting in a Zn_4 tetrahedron. Both Cu1 and Zn1 occupy a $\bar{4}3m$ special position in the crystal. To the best of our knowledge **1a/1b** are the first molecular compounds containing an unsupported Cu–Zn bond (2.498(2) Å). The only reported complex with a Cu–Zn contact is $[Zn\{(p-CH_3CO_2)(salpd-\mu-O,O')Cu\}_2]$ (salpd = propane-1,3-diylbis(salicylideneiminato)) with a Cu–Zn distance of 3.038(2) Å, which is clearly a non-bonding contact.¹⁷ The bond angles at copper are close to the ideal tetrahedral angle. In the crystal, the Cp/Cp* ligands are severely disordered by symmetry (see SI). The Zn–Cp*_{centroid} / Zn–Cp_{centroid} distances (2.05 Å) are well comparable with the parent compound $[Zn_2Cp^*_2]$ (2.04 Å).¹⁸ The Cu–C1 distance of 1.89(1) Å is comparable to the average Cu–CN^tBu distances found in the literature (1.91 Å). Notably, only one compound exhibiting a Zn–CN^tBu unit with a Zn–C bond length of 2.13 Å was structurally characterized, supporting our Cu/Zn assignment in the structure refinement (*vide supra*).¹³ Most interestingly, the structural motif of a $[Cu_4Zn_4]$ tetrahedral star is also found in the structure of the famous γ -brass phase Cu_5Zn_8 where an inner Zn_4 tetrahedron is surrounded by an outer Cu_4 tetrahedron, which is the "inverse" metal core to **1a/1b**.¹⁹ The metal-metal distances in γ -brass are 2.704(1) Å for the "inner" (Zn_4) tetrahedron and 4.319(1) Å for the "outer" (Cu_4) tetrahedron with a Cu–Zn distance of 2.611(1) Å, which considerably widened with respect to the distances observed in **1a/1b**: 2.462(4) Å for the "inner" (Cu_4) tetrahedron and 4.167(1) Å for the "outer" (Zn_4) tetrahedron with a Cu–Zn distance of 2.493(2) Å.¹⁹ DFT calculations²⁰ on the two models $[(CuCNMe)_4(ZnCP)_4]$ and $[(ZnCNMe)_4(CuCP)_4]$ (Me for ^tBu and Cp for Cp*; Table S8) confirm the Cu vs Zn location assignment, the former being much more stable than the latter (by 2.05 eV). A better agreement with the experimental metal-metal and metal-ligand bond distances, as well as with the $\nu(CN)$ stretching vibration frequency (2268 cm^{-1} vs. 2317 cm^{-1}) is also found for $[(CuCNMe)_4(ZnCP)_4]$. The values of the Cu–Cu and Cu–Zn Wiberg bond indices (0.102 and 0.151 respectively) are consistent with significant covalent bonding within the Cu_4Zn_4 framework. This bonding is largely operated by eight metallic σ -type hybrids of large 4s character which combine into 4 occupied bonding skeletal orbitals and 4 vacant antibonding ones according to the MO interaction diagram shown in Figure S8. The resulting HOMO-LUMO gap (3.57 eV) is large. This closed-shell situation is maintained when the four CNMe ligands are removed, indicating that they should be counted as neutral in the Jellium electron counting model (see below). Thus, there are 4 electron pairs to ensure delocalized bonding along the 16 metal-metal contacts. The four bonding orbitals span into a_1 , b_2 and e irreducible representations in the D_{2d} molecular symmetry. The near-degeneracy and shape similarity of the b_2 and e orbitals (see Figure S8) indicate that in the pseudo- T_d symmetry of the molecule, these four orbitals span into a_1 and t_2 .

In summary, **1a/1b** with a $[Cu_4Zn_4]$ core represent the first examples of molecular compounds containing Cu–Zn bonds. The metal core of the clusters is composed of superimposed Cu_4 and Zn_4 tetrahedra, which represents the "inverse" structure of a

structural motif found in γ -brass, Cu_5Zn_8 . This swapped Cu and Zn positions is assigned to the preference of the Cp*/CN^tBu binding to Zn and Cu respectively. We suggest rationalizing this composition and structure and its preferred formation with respect to alternatives within the unified superatom concept based on the jellium model for clusters of s/p metals (e.g. coinage metals, closed d^{10} sub shell).^{21, 22} For a spherical, highly symmetric ligand protected, molecular cluster $\{[M_m]L_sX_n\}^q$ (q = charge, L = electronically neutral weakly coordinating ligand; X = electronegative, electron withdrawing ligand) shell closing is expected for cluster valence electrons $cve = 2, 8, 18, 34, \dots$ (degenerate spherical jellium states $1S^2 1P^6 1D^{10} 2S^2 1F^{14}$, etc.). Regarding Cp* as one electron withdrawing X and CN^tBu as neutral L and taking into account the effective valence 1 for Cu and 2 for Zn the value $cve = 8$ is obtained for **1a/1b** ($1S^2 1P^6$ shell closing, which in T_d symmetry corresponds to the $a_1^2 t_2^6$ cluster electronic configuration discussed above). Thus, **1a/1b** can be described as ligand protected superatom clusters. The tetra capped tetrahedral structure adopted by the Cu_4Zn_4 core is also the most stable structure predicted by the simple Hückel theory for any 8-orbital/8-electron system.

Acknowledgements

This work was funded by the DFG (Fi-502/23-2). K.F. and H.B. are grateful for a FCI scholarship (<https://www.vci.de/fonds>) and for the support by the RUB Research School (<http://www.research-school.rub.de>). We thank the Linden CMS GmbH for support in mass spectrometry. JYS thanks the Institut universitaire de France for support.

Notes and references

- ^a *Inorganic Chemistry II, Ruhr-University Bochum, Universitätsstraße 150, 44801 Bochum, Germany. E-mail: roland.fischer@rub.de*
- ^b *Institut des Sciences Chimiques de Rennes - UMR 6226 Université de Rennes 1, 35042 Rennes Cedex, France*
- † Electronic Supplementary Information (ESI) available: [details of any supplementary information available should be included here]. See DOI: 10.1039/b000000x/
- ‡ Experimental: All manipulations were carried out using standard Schlenk and glove box methods. All solvents were degassed, dried and saturated with Ar prior to use.
- To a mixture of 150 mg $[CpCuCN^tBu]$ (0.708 mmol) and 285 mg $[Zn_2Cp^*_2]$ (0.708 mmol) 4 ml toluene were added whereas the solution immediately turned dark red. The solution was stirred for a period of one hour at room temperature. The solvent was removed under reduced pressure and the crude product washed with 2 portions of *n*-hexane (3 ml each). The crude product was dried in vacuum and 2 ml of toluene were added. Dark red cubic crystals suitable for single crystal X-ray measurements were collected after storage at -30 °C.
- ¹H NMR (C_6D_6 , 25 °C, ppm): $\delta = 1.24$ (36H, CN^tBu (**1a**)), 1.31 (9H, CN^tBu (**1b**)), 1.32 (27H, CN^tBu (**1b**)), 2.36 (45H, C_5Me_5 (**1b**)), 2.37 (60H, C_5Me_5 (**1a**)), 6.37 (5H, Cp (**1b**)).
- Elemental analysis (%) ($C_{57.5}H_{91}N_4Cu_4Zn_4$) calcd: Cu 18.77, Zn 19.31 found: Cu 19.32, Zn 20.52.
- LIFDI-MS: $m/z = 1424, 1389, 1319, 1306, 1188, 1170, 1107, 1091, 1040, 1022, 1010, 956, 893, 809, 746, 694$ (assignment SI Figure S4).
- IR: 2937, 2880, 2829, 2104, 1462, 1415, 1385, 1358, 1249, 1192, 1076, 1006, 853, 790, 744, 723, 690, 582, 545, 501, 461, 442 cm^{-1} .
- X-Ray Crystallography. Details of the single crystal structure measurement and refinement of **1a/b** are given in the supporting information to this article. CCDC 985016 contains the supplementary

crystallographic data for this paper. These data can be obtained free of charge from the Cambridge Crystallographic Data Centre via www.ccdc.cam.ac.uk/data_request/cif

- 5 1. R. Ferrando, J. Jellinek and R. L. Johnston, *Chem. Rev.*, 2008, **108**, 845-910.
2. J. Hambrock, M. K. Schroeter, A. Birkner, C. Woell and R. A. Fischer, *Chem. Mater.*, 2003, **15**, 4217-4222.
- 10 3. M. Cokoja, H. Parala, M. K. Schroeter, A. Birkner, M. W. E. van den Berg, K. V. Klementiev, W. Gruenert and R. A. Fischer, *J. Mater. Chem.*, 2006, **16**, 2420-2428.
4. R. E. Cable and R. E. Schaak, *Chem. Mater.*, 2007, **19**, 4098-4104.
5. K. Schuette, H. Meyer, C. Gemel, J. Barthel, R. A. Fischer and C. Janiak, *Nanoscale*, 2014, **6**, 3116-3126.
- 15 6. T. Bollermann, C. Gemel and R. A. Fischer, *Coord. Chem. Rev.*, 2012, **256**, 537-555.
7. S. Gonzalez-Gallardo, T. Bollermann, R. A. Fischer and R. Murugavel, *Chem. Rev.*, 2012, **112**, 3136-3170.
- 20 8. T. Cadenbach, T. Bollermann, C. Gemel, I. Fernandez, M. von Hopffgarten, G. Grenking and R. A. Fischer, *Angew. Chem., Int. Ed.*, 2008, **47**, 9150-9154.
9. T. Bollermann, M. Molon, C. Gemel, K. Freitag, R. W. Seidel, M. von Hopffgarten, P. Jerabek, G. Frenking and R. A. Fischer, *Chem. Eur. J.*, 2012, **18**, 4909-4915.
- 25 10. T. Bollermann, K. Freitag, C. Gemel, R. W. Seidel and R. A. Fischer, *Organometallics*, 2011, **30**, 4123-4127.
11. C. Zybilla and G. Mueller, *Organometallics*, 1987, **6**, 2489-2494.
12. T. Kruck and C. Terfloth, *Chem. Ber.*, 1993, **126**, 1101-1106.
- 30 13. M. Bochmann, G. C. Bwembya and A. K. Powell, *Polyhedron*, 1993, **12**, 2929-2932.
14. N. P. Mankad, D. S. Laitar and J. P. Sadighi, *Organometallics*, 2004, **23**, 3369-3371.
15. Q.-H. Wei, G.-Q. Yin, L.-Y. Zhang, L.-X. Shi, Z.-W. Mao and Z.-N. Chen, *Inorg. Chem.*, 2004, **43**, 3484-3491.
- 35 16. J. Beck and J. Straehle, *Angew. Chem.*, 1985, **97**, 419-420.
17. C. Fukuhara, K. Tsuneyoshi, N. Matsumoto, S. Kida, M. Mikuriya and M. Mori, *J. Chem. Soc., Dalton Trans.*, 1990, 3473-3479.
18. I. Resa, E. Carmona, E. Gutierrez-Puebla and A. Monge, *Science*, 2004, **306**, 411.
- 40 19. O. Gourdon, D. Gout, D. J. Williams, T. Proffen, S. Hobbs and G. J. Miller, *Inorg. Chem.*, 2007, **46**, 251-260.
20. PBE0/Def2-TZVP level. Details of the calculations are provided in the SI.
- 45 21. H. Haekkinen, *Chem. Soc. Rev.*, 2008, **37**, 1847-1859.
22. M. Walter, J. Akola, O. Lopez-Acevedo, P. D. Jadzinsky, G. Calero, C. J. Ackerson, R. L. Whetten, H. Gronbeck and H. Hakkinen, *Proc. Natl. Acad. Sci.*, 2008, **105**, 9157-9162.

50

Entry for Table of Contents

55 Kerstin Freitag, Hung Banh, Christian Gemel, Rüdiger W. Seidel, Samia Kahlal, Jean-Yves Saillard and Roland A. Fischer

First examples of structurally characterized “molecular brass”

60 The first examples of structurally characterized “molecular brass”, $[(\text{CuCN}^t\text{Bu})_4(\text{ZnCp}^*)_4]$ and $[(\text{CuCN}^t\text{Bu})(\text{ZnCp}^*)_3\text{ZnCp}]$ exhibit the structural motif of a $[\text{Cu}_4\text{Zn}_4]$ tetrahedral star, which is inversely found in the γ -brass phase Cu_5Zn_8 .

65

